Article

Higgs and BSM Physics at the Future Muon Collider

Roberto Franceschini *[ID] and Mario Greco *

Dipartimento di Matematica e Fisica, Università degli Studi Roma Tre and INFN, Sezione di Roma Tre, Via della Vasca Navale 84, I-00146 Rome, Italy
* Correspondence: roberto.franceschini@uniroma3.it (R.F.); mario.greco@roma3.infn.it (M.G.)

Abstract: We describe recent work on the physics of the Higgs boson and breaking of the electroweak symmetry at future muon colliders. Starting from the low-energy muon collider at the Higgs boson pole we extend our discussion to the multi-TeV muon collider and outline the physics case for such machines about the properties of the Higgs boson and physics beyond the Standard Model that can be possibly discovered.

1. Introduction

The opportunities offered by the realization of muonic beams have been realized long ago and the interest for this idea has been high for decades [1–5]. More recently, there has been more interest in the possibility of constructing a $\mu^+\mu^-$ collider [6–10]. Various surveys of the physics opportunities at such a collider have been made, see for example Refs. [11,12]. It follows that a $\mu^+\mu^-$ collider can essentially explore all the same physics that is accessible at an e^+e^- collider of the same energy, but differently from the past, the time for a jump towards a future muon collider may now be finally ripe, as the possibilities for other more conventional types of colliders are shrinking and we are forced to think about bold and innovative new types of machines. On the other hand, the Higgs boson discovery at the LHC in 2012 [13,14] has opened a new era of particle physics and its properties absolutely need to be analyzed with great precision and fully understood. The focus of any Higgs physics program is the question of how the Higgs boson couples to other Standard Model (SM) particles. Within the SM itself, all the couplings are uniquely determined, but possible new physics beyond the SM will modify these couplings in different ways, as the Higgs, for example, could be the portal to other gauge sectors. Then the Muon Collider (MC) opens the particularly interesting possibility of direct *s*-channel Higgs production. In addition, the MC is also a possible option for the next generation of high-energy collider machines, as it would allow achieving the highest energy frontier in lepton collisions, because muons do not suffer significant energy losses due to synchrotron radiation and therefore could be accelerated up to multi-TeV collision energies.

Among many candidates of Higgs factories [15,16] the possibility of resonant production is especially important. The muon collider Higgs factory could produce the Higgs particle in the *s*-channel and perform an energy scan to map out the Higgs resonance line-shape at a few MeV level. This approach would provide in principle the most direct measurement of the Higgs boson total width and the Yukawa coupling to the muons and other SM particles. However, the extremely narrow width of the Higgs boson ($\Gamma/M = 3.4 \times 10^{-5}$) makes the resonant production rate very subject to any effect that shifts the collision center-of-mass energy of the lepton collider. Indeed, there are two effects convoluted with the Higgs resonance production, the Beam Energy Spread (BES) and additional Initial State Radiation (ISR) corrections to the hard process which put

severe limitations on the observed production cross-section [17], by modifying the naive expectation of a sharp Breit–Wigner for the Higgs resonance production.

The aim of the present paper is two-fold. First, we will review the Higgs *s*-channel resonance production, with a detailed discussion of the ISR effects, which play an important role in reducing the line-shape cross-section, and of the limitations from the BES to allow the appropriate precision of the experiments. In addition, we will also discuss the background expectations of resonance for the main expected final states.

Besides the possibility to make a Higgs boson factory using muon beams, the possibility to store and accelerate large quantities of muons opens the road to conceiving a high-energy lepton collider with circulating beams. In this work we will explore possible studies of the Higgs boson properties and associated new physics that are enabled by a high-energy muon collider with center-of-mass energy in the multi-TeV regime.

The opportunities enabled by the availability of high-energy bright muon beams are unique in the landscape of future colliders. In fact, most of the current projects of lepton collider operating at center- of-mass energy well above the thresholds of SM states are linear colliders. The reason is that electron and positron beams emit too large amounts of synchrotron radiation if put in a circular orbit, therefore the linear collider option is the only viable one if one wants to tame synchrotron radiation. To reach multi-TeV center-of-mass energy in linear colliders very innovative accelerator designs [18] have been studied and tested in demonstrator facilities [19]. Still, it seems hard to go beyond the 3 TeV center-of-mass energy of the latest CLIC project stage. Despite the great amount of work to optimize the innovative two-beam acceleration scheme of CLIC, it remains very difficult to reach such large center-of-mass energy without exceeding affordable amounts of wall-plug power requirements. Indeed the 3 TeV stage of CLIC is estimated to require a yearly consumption of electric energy in the range of a few times the expenditure of the future HL-LHC [20].

The power-hungry character of linear electron–positron colliders is not an isolated case in the landscape of particle colliders [21,22]. In fact, power requirements are a crucial bottleneck for the development of pp collider as well as lower energy e^+e^- colliders on circular tunnels. For e^+e^- circular colliders this is obviously the consequence of the synchrotron radiation we already mentioned. Even the most ambitious programs under discussion, the CEPC [23,24] and *FCC*-ee projects [25], do not dare to consider running above the $t\bar{t}$ threshold. Proton colliders also struggle with synchrotron radiation as it is one of the main ways to heat the superconducting magnets, and significant power must be used to shield the magnets [26,27] and keep them at the operating temperature.

The possibility to circulate and handle muonic beams creates a road towards leptonic collision in the multi-TeV center-of-mass energy ballpark, with manageable synchrotron radiation and affordable power costs [10,28]. Therefore, a high-energy muon collider might be the pioneering project we need to set a new course for future explorations in high-energy physics. The jump in achievable center- of-mass energy can be compared to the terrific progress that followed milestone advances in particle accelerators such as the introduction of beam–beam particle anti-particle collisions [29–31], the use of superconducting materials in RF frequencies [32] or stochastic cooling for $p\bar{p}$ collisions [33].

Then we will examine the potential to explore new physics using these multi-TeV energy muon collisions using direct searches of new states, as well as indirect signals. Furthermore, we will consider the possibility to stress test the SM using the copious production of SM states, e.g., Higgs bosons and third-generation quarks, measuring accurately properties of these SM states.

In Section 2 we discuss the possibility of the *s*-channel resonant Higgs production and the parameterization of the BES and ISR effects. Then we also discuss in detail their impact on the signal and the background for the main expected final states and on the global fits of Higgs properties. In Section 3 we present the possibility to investigate Higgs physics and in particular BSM physics in the Higgs sector at a multi-TeV muon collider. In this section, we outline the several strategies that can be deployed at a multi-TeV muon collider thanks to the large momentum transfer available in reactions involving the beam particles and

the low momentum ones from the "partons" within the scattering muons. We present an outlook and our conclusions in Section 4.

2. Low-Energy Muon Collider

2.1. Higgs Boson Resonant Production

The possibility of *s*-channel resonant Higgs production is especially interesting [11] and indeed a muon collider can produce the Higgs boson resonantly at a reasonable rate. In the SM this measurement could probe the Higgs bosons width and the muon Yukawa directly. The clean environment of the lepton collider also enables precision measurement for many exclusive decays of the Higgs boson. This is particularly important also in the case of SUSY extensions of the SM, where the Higgs sector contains at least two Higgs doublets and the resulting spectrum of physical Higgs fields includes three neutral Higgs bosons, the CP-even h_0 and H_0 and the CP-odd A_0. The couplings of the MSSM Higgs bosons to fermions and vector bosons are determined by $\tan \beta$ and the mixing angle α between the neutral Higgs states h_0 and H_0. In addition, all the Higgs bosons are produced in sufficient abundance in the *s*-channel muon-antimuon collisions to allow their detection for most of the parameter space. The Higgs boson widths are then crucial parameters, and for this study the muon collider is particularly suitable, also for providing tests of lepton universality of the Higgs couplings.

From the accelerator's point of view, after the pioneering studies of the Muon Ionization Cooling Experiment (MICE) [34] , new suggestions have been recently put forward to realize a muon collider. First the proposal by C. Rubbia [8,35], with a collider ring of radius of about 50 m, which however also requires a powerful muon cooling process. Then, more recently, a low emittance muon accelerator (LEMMA) [36,37] has been suggested, using a positron beam on target, with the muons being produced in the electron–positron annihilation almost at rest, and the muon cooling is not necessary.

The extremely narrow width of the Higgs boson of about 4.1 MeV as predicted by the SM, makes the resonant production rate subject to any effect that shifts the collision c.m. energy of the lepton collider. Then there are two important effects related with the Higgs resonance production, the BES and the ISR corrections that make important modifications to the naive expectations. In a previous work [17] the convoluted effects of both BES and ISR have been studied over the Breit–Wigner resonance for Higgs production at the muon collider. Their impact in different scenarios for both the Higgs signal and SM background has been considered. That study provides an improved analysis of the proposed future resonant Higgs factories and is also helpful for our understanding of the target accelerator design. In the following we will review those results that have important implications for the experiments and for the beam geometry design.

Multiple soft photon radiation is an important effect which must be taken into account when a narrow resonance is produced in the annihilation channel in lepton colliders. The first very clear example of such effect has been with the historical observation of J/Psi production in e^+e^- annihilation [38] and the origin was soon discussed in very great detail [39], and also later for the case of the Z-boson production [40]. As a result, a correction factor $\propto (\Gamma/M)^{4\alpha/\pi \log(2E/m)}$ modifies the lowest order cross-section, where M and Γ are the mass and width of the *s*-channel resonance, $W = 2E$ is the total initial energy and m is the initial lepton mass. Physically this is understood by saying that the width provides a natural cut-off in damping the energy loss for radiation in the initial state. Very precise calculation techniques for these QED effects have been developed for LEP experiments, where in addition to multi-photon radiation finite corrections have been added, by including, at the least, up to two-loop effects, see for example Ref. [41]. In the case of muon colliders, in particular for Higgs boson production studies, those effects were not emphasized sufficiently in the past, and only recently their importance has been pointed out [42,43] for the experimental study of the Higgs line-shape as well as for the machine design of the initial BES. In particular, the estimates of the reduction factors of the Higgs production cross-sections, of order of 50% or more, depending upon

the machine energy spread, given in Ref. [42], have been confirmed in Refs. [17,43], where the calculation techniques developed at the time of LEP experiments have been used, in order to estimate the expected precision of the theoretical results.

Within the general formalism of the lepton structure functions, first introduced in Ref. [44], and later improved for LEP experiments, defining the probability distribution function $f_{\ell\ell}^{\text{ISR}}(x)$ for the hard collision energy $x\sqrt{\hat{s}}$, then the hard collision cross-section is written as

$$\sigma(\ell^+\ell^- \to h \to X)(\hat{s}) = \int dx \, f_{\ell\ell}^{\text{ISR}}(x;\hat{s})\hat{\sigma}(\ell^+\ell^- \to h \to X)(x^2\hat{s}), \tag{1}$$

where x is the fraction of the c. m. energy at the hard collision with respect to the beam energy before the collision. Various approximations for the distribution function in the literature have been discussed in Ref. [17], we will show the results obtained using the distribution function given in Ref. [41] which contains the full exponentiated term and the complete $O(\alpha)$ and $O(\alpha^2)$ terms.

In addition, the observable cross-section is given by the convolution of the energy distribution delivered by the collider. We assume that the lepton collider c.m. energy ($\sqrt{s}$) has a flux L distribution

$$\frac{dL(\sqrt{s})}{d\sqrt{\hat{s}}} = \frac{1}{\sqrt{2\pi}\Delta} \cdot \exp\left[\frac{-(\sqrt{\hat{s}} - \sqrt{s})^2}{2\Delta^2}\right], \tag{2}$$

with a Gaussian energy spread $\Delta = R\sqrt{s}/\sqrt{2}$, where R is the percentage beam energy resolution. Then the effective cross-section is

$$\sigma_{\text{eff}}(s) = \int d\sqrt{\hat{s}} \, \frac{dL(\sqrt{s})}{d\sqrt{\hat{s}}} \, \sigma(\ell^+\ell^- \to h \to X)(\hat{s}) \tag{3}$$

For $\Delta \ll \Gamma_h$, the line-shape of a Breit–Wigner resonance can be mapped out by scanning over the energy $\sqrt{s}$ as given in the first equation. For $\Delta \gg \Gamma_h$ on the other hand, the physical line-shape is smeared out by the Gaussian distribution of the beam energy spread and the signal rate will be determined by the overlap of the Breit–Wigner and the luminosity distributions.

As a consequence of the ISR, a very significant phenomenon is the "radiative return" to a lower mass resonance. Despite the beam collision energy is above a resonance mass, after ISR effects, the hard collision center-of-mass energy "returns" to the resonance mass and hits the Breit–Wigner enhancement again. This mechanism can be used to effectively produce lighter resonances without scanning the beam energy. On the other hand, when running at 125 GeV in a lepton collider the amount of "radiative return" Z bosons produced constitutes a large background for Higgs studies. One can easily see that different parameterizations of the ISR effects yield significantly different amount of "radiative return" Z production rate. This consideration clearly shows the importance of a proper accurate treatment in evaluating the ISR effect.

2.2. Numerical Results on the ISR and BES on Resonance

The ISR effects, as discussed in the previous section, are very important and need to be convoluted with the finite BES. We summarize numerically their combined effect in the Higgs boson production measurements in this section [17].

In Table 1 we show the reduction effects for the resonance production of the SM Higgs boson at 125 GeV including BES and ISR. The resonance production rate is reduced by a factor of about 2 with the inclusion of ISR effect. Independently, the production rate would be reduced by factors of 4.2 and 1.7 for beam spread of 0.01% and 0.003% respectively. The total reduction after the convolution of the beam spread and the ISR effect is 7.1 and 3.2 for the two-beam spread scenarios, respectively. A convenient analytical formula for

evaluating the reduction factor on the peak as a function of the resonance width and the machine energy spread, has been given in Ref. [42].

Table 1. Effective cross-sections in units of pb at the resonance $\sqrt{s} = m_h = 125$ GeV, with Breit–Wigner resonance profile alone, with ISR alone, with BES alone for two choices of beam energy resolutions, and both the BES and ISR effects included.

σ(BW)	ISR Alone	R (%)	BES Alone	BES+ISR
71 pb	37	0.01	17	10
		0.003	41	22

The resulting line-shape from Ref. [17] is shown in Figure 1 (left panel for the $\mu^+\mu^-$ collider) for various setups of the parameters. For the reader's convenience we also show (right panel) the ISR and BES results of Ref. [17] for an electron–positron collider. The sharp Breit–Wigner resonance is in solid blue lines. The BES will broaden the resonance line-shape with a lower peak value and higher off-resonance cross-sections, as illustrated by the green curves. The solid lines and dashed lines represent the narrow and wide BES of 0.003% and 0.01%, respectively. In red lines we show the line shapes of the Higgs boson with both the BES and the ISR effect. The crucial role played by the numerical value of the BES parameter R is shown in Figure 1. When $R \gg 0.003\%$ the resonance signal is almost absent. This is clearly shown also in Figure 2 for $R = 0.1\%$. The above analysis clearly indicates that a muon collider resonant Higgs factory makes sense only if the initial beams energy spread is of order of the Higgs width.

In addition to the Higgs signal, an important issue of phenomenological interest is the question of the expected background in the various Higgs decay channels. This is related to the tail of the Z-boson production in the lepton annihilation. This issue has been discussed in detail in Ref. [17]. We will report here the main conclusions. The main search channels will be the exclusive mode of $b\bar{b}$ and WW^*. For the $b\bar{b}$ final state the main background is from the off-shell Z/γ s-channel production. The ISR effect does increase the on-shell process $Z \to b\bar{b}$ background through the radiative return by a factor of seven. This can be reduced by imposing an invariant mass cut of about 100 GeV which leads to around 20% increase in such background compared to the tree-level estimate. Alternatively, one can foresee a cut on the angle between the two b-jets, which could be measured more precisely than the invariant mass.
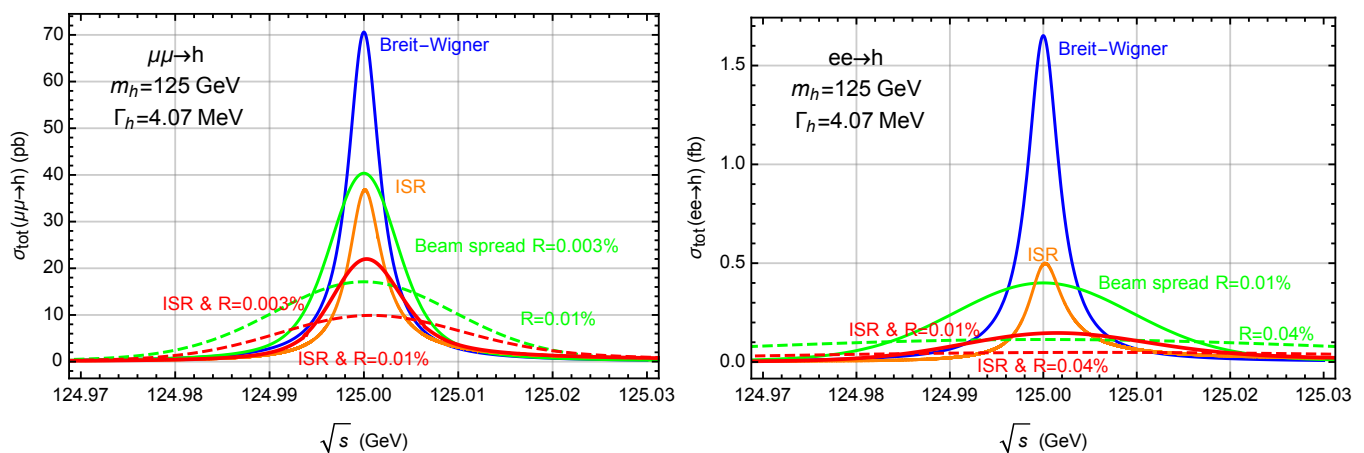

Figure 1. The line shapes of the resonances production of the SM Higgs boson as a function of the beam energy $\sqrt{s}$ at a $\mu^+\mu^-$ collider (**left panel**) and an e^+e^- collider (**right panel**). The blue curve is the Breit–Wigner resonance line-shape. The orange line-shape includes the ISR effect alone. The green curves include the BES only with two different energy spreads. The red line shapes take into account all the Breit–Wigner resonance, ISR effect and BES in solid and dashed lines, respectively.
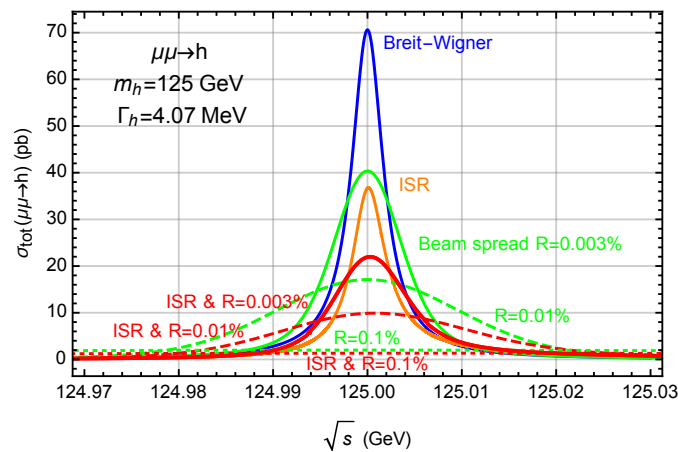
Figure 2. Same as in Figure 1, with R = 0.1%.

Beyond the $b\bar{b}$ final state, another major channel for muon collider Higgs physics is the WW^* channel. In this channel the background from the SM process is quite small. The ISR effect introduces no "radiative return" for such process. Consequently, the background rate does not change from the tree-level estimate. We summarize in Table 2 the on-shell Higgs production rate and background rate in these two leading channels with the inclusion of the ISR and BES effects. We can see from the table that at the muon collider Higgs factory, the signal to background ratio is pretty large and the observability is simply dominated by the statistics.

Table 2. Signal and background effective cross-sections at the resonance $\sqrt{s} = m_h = 125$ GeV in pb, for two choices of beam energy resolutions R and two leading decay channels with ISR effects taken into account, with the SM branching fractions $\mathrm{Br}_{b\bar{b}} = 58\%$ and $\mathrm{Br}_{WW^*} = 21\%$. For the $b\bar{b}$ background, a conservative cut on the $b\bar{b}$ invariant mass to be greater than 100 GeV is applied.

R (%)	$\mu^+\mu^- \to h$ σ_{eff} (pb)	$h \to b\bar{b}$		$h \to WW^*$	
		σ_{Sig}	σ_{Bkg}	σ_{Sig}	σ_{Bkg}
0.01	10	5.6	20	2.1	0.051
0.003	22	12		4.6	

2.3. Outlook on Low-Energy Options

We have discussed the s-channel resonant Higgs production in a future muon collider together with the effects from the initial state radiation and the beam energy spread. We have quantified their impact for different representative choices of the BES for both the Higgs signal in its main decay modes and the corresponding SM background. We have shown that the BES effect is potentially the leading factor for the resonant signal identification, and it alone reduces the on-resonance Higgs production cross-section by a factor of 1.7 (4.2) for a muon collider with $R = 0.003\%$ ($R = 0.01\%$). Then the ISR effect alone reduces the on-resonance Higgs production cross-section by a factor of about 2. The total reduction factors for the on-resonance Higgs production cross-section after convoluting the BES and ISR effects are 3.2 (7.1) for a muon collider with $R = 0.003\%$ ($R = 0.01\%$). Therefore, the BES parameter R plays a crucial role and the above analysis clearly indicates that a muon collider resonant Higgs factory makes sense only if the initial beams energy spread is of order of the Higgs width. In addition, the background for the $h \to b\bar{b}$ channel is increased by a factor of seven due to the "radiative return" of the Z boson and a cut on the minimal $b\bar{b}$ invariant mass of 100 GeV reduces such background, resulting in an increase of the tree-level estimate of the background by 20%. Then both the $h \to b\bar{b}$ and $h \to WW^*$ contribute to the signal sensitivity.

Significant efforts are needed to achieve these ambitious targets on the beam parameters for a muon collider Higgs boson factory at the Higgs boson pole. Given the size of the effort needed it is important to carefully gauge the reward that one could obtain in the knowledge of the Higgs boson from such Higgs boson factory. Considering realistic integrated luminosities $O(fb^{-1})$ the Higgs pole muon collider would produce at best a fraction of 10^5 Higgs bosons. Statistical uncertainties from such a data set can lead to couplings determinations in the ballpark of 1% precision for the most abundant Higgs boson decay channels, thus potentially improving on the most optimistic Higgs boson couplings determination that the HL-LHC could give [45].

The Higgs pole muon collider Higgs boson factory would also have the great advantage over the HL-LHC to be able to measure the Higgs boson width directly [17,46–49]. Such a measurement is one of the few possible ways to obtain absolute measurements on the Higgs couplings, therefore would be a cornerstone for our knowledge of the Higgs boson and will have impact on any future study of the Higgs boson. As a matter of fact, even in the presence of a large data sets, e.g., the $O(10^6)$ Zh pairs produced at the circular e^+e^- machines at the Zh threshold considered in Refs. [50–52], the best known quantities will be dimensionless ratios, e.g., ratios of rates or ratios of branching fractions, whereas we will have significantly worse knowledge of the overall scale of these rates and absolute Higgs couplings. Remarkably, the knowledge of an absolute coupling scale from the Higgs boson width measurement that can be carried out at a muon collider Higgs boson pole factory could come quite close to what is doable by measuring the total Zh rate and using the recoil method in hadronic Z and leptonic Z boson events, with no requirements on the decay of the Higgs boson at e^+e^- factories operating at 240 GeV and above. The actual result on the Higgs boson width and its impact on the overall determination of the Higgs boson couplings is an active subject of study [53]. Preliminary results [49,53] indicate that a clean extraction of the Higgs boson width can lead to couplings determinations that may be only slightly inferior to the performance of a Higgs boson factory at the Zh threshold [50–52] or at higher energies [54].

3. High-Energy Muon Collider

3.1. First of a New Kind

The idea of a high-energy muon collider has been put forward since decades [1–5] and the possibility to use muon beams to go to the highest energies is definitely not new. Differently from the past, the time for a jump towards a future muon collider may now be finally ripe, as the possibilities for other more conventional types of colliders are shrinking, and we are forced to think about bold and innovative new types of machines.

In fact, future electron–positron circular machines and pp colliders are essentially based on the same type of technology that enabled the Large Hadron Collider (LHC) and the Large Electron–Positron collider (LEP). Of course, improvements have been possible over the years of operation of these types of machines and will still be possible in the future application of these technologies [55,56], but it is fair to say that presently discussed future e^+e^- and pp colliders [52] are mostly bigger and not fundamentally different from their predecessors.

The developments necessary to build these bigger e^+e^- and pp machines, e.g., in superconductors technology [57,58], represent great challenges and might have enormous societal and technological impact. These advances are definitely worth a strong R&D program, as indicated by the recent update of the European Strategy for Particle Physics [59,60]. Still, these futuristic e^+e^- and pp machines will be "just" more powerful versions of machines we have already built.

On the contrary, a high-energy muon collider will be the first of a new kind of machines and will open the way to a novel investigation of fundamental interactions at the shortest distances, significantly improving over the physics capabilities of more traditional machines in most kind of investigations. The recent surge of phenomenological studies on the physics case of the muon collider [61–89] is a proof of the enormous interest on this machine.

In the following we will outline the tracks along which a high-energy muon collider can investigate new physics at the energy frontier. We will highlight the strengths of the investigations enabled by high-energy muon collisions and we will also highlight crucial requirements that need to be met by this kind of machine or risk to jeopardize the outcome of these investigations.

3.2. Multiplexing the Search for New Physics

A distinctive feature of high-energy muon colliders in searching for new physics is that they can operate different search modes and it is possible to obtain very strong bounds from different types of searches.

For a quick categorization of search modes that can be pursued at a high-energy muon collider we can divide searches in:

- Direct production of new physics, e.g., the on-shell production of new states $\ell^+\ell^- \to \chi\chi$ where χ is a new physics particle, for instance, a dark matter particle;
- Indirect effects from off-shell new physics, e.g., the modification to the angular distribution of $\ell^+\ell^- \to f\bar{f}$ Drell–Yan processes due to contact interactions $\bar{\psi}_\ell\psi_\ell\bar{\psi}_f\psi_f$ beyond the SM;
- Copious production of SM states in (effective) $2 \to 1$ annihilations, $2 \to 2$ scatterings, or 3-body and multi-body productions. These include for instance the effective W boson annihilation to produce Higgs bosons in $\ell^+\ell^- \to \nu\nu h$, $\ell^+\ell^- \to t\bar{t}$ and $\ell^+\ell^- \to t\bar{t}h$ processes.

In all these search modes a high-energy muon collider will result in significant advances compared to the HL-LHC and, in most cases, even in comparison to proposed ambitious future collider projects.

We will briefly discuss examples of these search strategies in the following. For now, we can highlight that the key feature of a high energy muon collider that enables all these search strategies is the possibility to have *both* a large center-of-mass energy *and* at the same time keep a relatively clean collision environment. A high-energy muon collider can operate as a clean lepton machine and at the same time have reach over the energy frontier comparable, if not superior, to hadronic machines.

Furthermore, a high-energy muon collision has the great operational advantage in that the searches outlined above can be pursued *at the same time*, without requiring dedicated runs or machine settings. Due to the largely unknown character of new physics this fact is very important, as it implies that the operation of a high-energy muon collider does not need to commit to one strategy ahead of time or to make hard choices in allocating machine run time or planning stages of its construction.

3.3. Direct Production of New Physics

Muons, being point-like particles, have the great advantage to make all their energy available to produce heavy final states. This needs to be contrasted with protons, for which we are forced to talk about partons and energy fractions carried by them from the very start of description of the collisions.

As muons carry electric and weak gauge charges, they are excellent initial states to produce any state, SM or BSM, that has electric or weak gauge charge. Assuming only these gauge interactions for new physics states, and barring any non-gauge interactions for the moment, we can compute cross-section for the production of heavy states at a high-energy muon collider. They are reported in Figure 3 as number of event at a 10 TeV collider for 10/ab integrated luminosity. The figure is taken from Ref. [72] and displays the result for a set of new physics states using a supersymmetric nomenclature, but without having in mind any supersymmetric model of sort. The name $\tilde{t}_L$ should just be read as a shorthand for the $SU(3) \otimes SU(2) \otimes U(1)$ gauge quantum numbers that in this case are $(3,2)_{1/6}$. We stress that only gauge interactions are considered in this result.
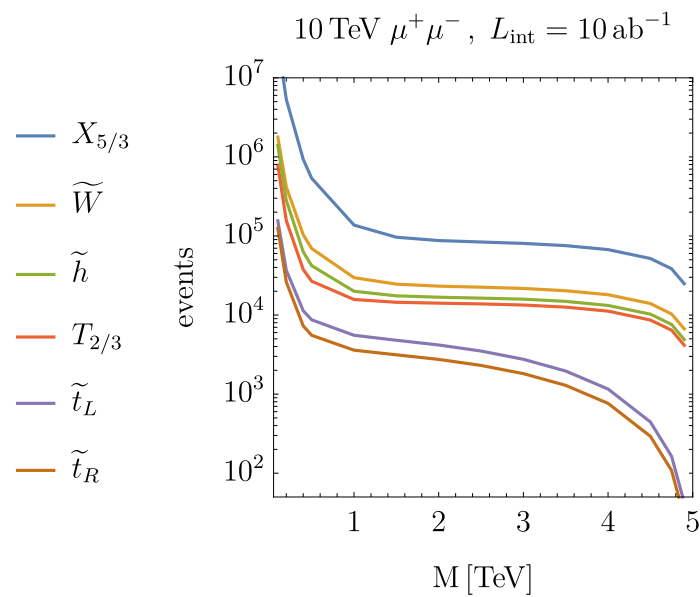
Figure 3. Rates for direct production of new states. The labels follow standard nomenclature of composite Higgs models and supersymmetric models. However, we computed cross-sections using only gauge interactions, whereas in these models each state may have specific model dependent interactions that can increase their production rate. Therefore our labels are shorthand for $SU(3) \otimes SU(2) \otimes U(1)$ charges: fermions $X_{5/3} \sim (3,2)_{7/6}$, $\widetilde{W} \sim (1,3)_0$, $\tilde{h} \sim (1,2)_{\pm 1/2}$, $T_{2/3} \sim (3,1)_{2/3}$ and scalars $\tilde{t}_L \sim (3,2)_{1/6}$, $\tilde{t}_R \sim (3,1)_{2/3}$.

The reported cross-section contains two main contributions: *(i)* the direct production in $2 \to 2$ Drell–Yan process; *(ii)* the production from gauge boson fusion from the flux of equivalent vector bosons that is part of the muon beam quantum structure, i.e., it follows from the $\mu \to W\nu$ or $\mu \to \gamma\mu$ and $\mu \to Z\mu$ splittings.

The Drell–Yan production is essentially given by the gauge couplings and the geometrical factors of the cross-section, so that for a particle with couplings of order $O(1)$ we expect a $2 \to 2$ cross-section

$$\sigma \simeq O(1) \, \text{fb} \cdot \left(\frac{10 \, \text{TeV}}{\sqrt{s}} \right)^2 . \tag{4}$$

This cross-section may be larger in the case of large multiplicities in the final state due to spin or color quantum numbers, hence scalars have smaller cross-sections than fermions and colored particles have larger particles than particles without color.

When the mass of the produced particle is light compared to the center-of-mass energy of the collider, it is possible to efficiently produce particles from collisions of equivalent bosons, e.g.,

$$WW \to \chi\chi,$$

from W boson radiated off the beams. In the collinear radiation approximation these collisions can be factorized, and we can talk about an effective W boson beam and effective W bosons fusion. This process suffers the decrease of the partonic luminosity of the W bosons at large WW center-of-mass energy. The flux of possible polarization states of W partons in the muon beam structure can be seen in Figure 4 from Ref. [82] and it roughly falls a fifth power of the WW center-of-mass energy tracker variable $\sqrt{\tau} = m_{WW}/\sqrt{s}$.
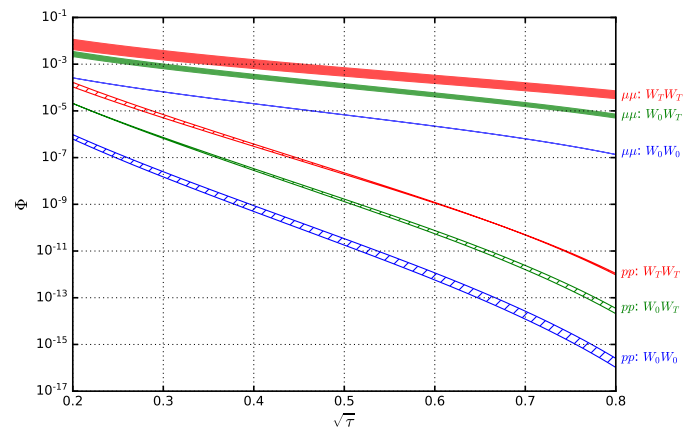
Figure 4. Partonic flux for transverse-transverse (red), transverse-longitudinal (green), longitudinal-longitudinal (blue) *W* boson in *pp* (hatched) and $\mu\mu$ (solid shading) collisions.

Clearly the boson fusion processes can give significant enhancements of the total rates for new physics states, but are largely subdominant to $2 \to 2$ Drell–Yan close to the kinematic reach of the machine. Therefore, the reach over the energy frontier of a high-energy muon collider can be estimated simply looking at the Drell–Yan rates. With this prescription in mind, it is clear that the mass reach of a muon collider for new physics states can be quite close to $\sqrt{s}/2$. The actual reach depends on how spectacular or subtle is the decay mode of the newly produced particles, but the relatively clean collision environment places us in favorable conditions to go after even somewhat subtle signatures. This should be contrasted with the typical situation of hadronic colliders in which it is relatively easy to hide copiously produced particles by just having them decay into soft enough final states that can be easily produced in SM reactions.

An educated guess for a model-independent comparison of pp and $\ell^+\ell^-$ direct reach for new physics can be found in Ref. [82]. The outcome is that a 14 TeV center-of-mass energy $\ell^+\ell^-$ collider can be as powerful to probe directly heavy new physics as a 100 TeV pp collider. Concrete studies for the production of heavy Higgs bosons weak doublets or singlets confirm an excellent sensitivity to the production of these states in vector boson fusion for singlets [87] and in pair production via gauge interactions or other associated productions for doublets [68].

It is important to stress that because of the expected cross-section for an electroweak Drell–Yan process in Equation (4), the luminosity requirement for a discovery with a O(10) new physics events is a rather low integrated luminosity of order O(10^{-2}) ab^{-1} for a 10 TeV machine. This is considerably below what has been found would be doable in the MAP study [9] for a proton-sourced muon collider and is largely below the luminosities consider even in "luminosity-hungry" linear $\ell^+\ell^-$ colliders [90]. In conclusion, the direct search for new physics is major driver towards increasing the attainable $\sqrt{s}$, but does not pose serious constraints for what concerns the luminosity of these machines.

3.4. Indirect Effects from Off-Shell New Physics

Indirectly testing new physics requires studying well measurable quantities for which precise and reliable predictions are available from theory. A classic example for leptonic colliders is the angular distributions of final states, which can reveal heavy new physics beyond the kinematic reach of the machine, e.g., a hint of heavy weak bosons from processes dominated by QED [91].

Although the accuracy of theoretical calculations available might change from now to the time of operation a high-energy muon collider, the possibility to measure accurately simple quantities such as total or fiducial rates can be largely anticipated today by just looking at the statistical uncertainties expected for the rates of interests. For a process

with cross-section σ we expect to collect a number of events $N = \sigma \cdot \mathcal{L}$, where $\mathcal{L}$ is the total luminosity collected at the experiment. As we are considering high-energy processes we can roughly estimate cross-sections by dimensional analysis $\sigma \sim 1/s$, where s is the characteristic energy scale of momentum transferred in the scattering and the exact coefficients are determined by the coupling constants of phase-space factors of each process. In particular, for a $2 \to 2$ scattering we gave the estimate Equation (4), which is valid for the production of SM as well as BSM states. According to this estimate, if we take a luminosity

$$\mathcal{L} = 10 \text{ ab}^{-1} \cdot \left(\frac{\sqrt{s}}{10 \text{ TeV}} \right)^2 \tag{5}$$

we obtain

$$N = \sigma \cdot \mathcal{L} = 10^4 \text{ events independently of } \sqrt{s}.$$

This number of events is apt to carry out precision measurements at the 1% level. Of course, the exact number of events usable in the measurement and the exact meaning of "precision" needs to be qualified further, but we find this estimate nevertheless useful as it poses a rough target for any plan to use a muon collider to carry out precision studies. Indeed, obtaining a smaller number of events would result in measurements at the O(10%) level which can hardly be called "precise".

To put these considerations on firm ground we need to compute the expected size of the effects from new physics. Taking into account that a machine running at center-of-mass energy $\sqrt{s}$ can directly produce and discover new particles with mass below $\sqrt{s}/2$ it makes sense to consider effects from new physics heavier, and possibly much heavier, than the direct production limit $\sqrt{s}/2$. The effects of these state-of-mass $M \gg \sqrt{s}$ can be encapsulated in several new interactions vertexes that are contact interactions among SM states, e.g., a four-fermion contact interaction such as that of the Fermi theory of weak interactions at energies well below the mass of the W boson. When we study reactions in which new contact interactions can mediate the scattering we obtain contributions to the scattering amplitude weighed by powers of

$$\epsilon = g^2 \left(s/M^2 \right). \tag{6}$$

As a result, the interference between SM and BSM sub-amplitudes contributes to the cross-section with an $\sqrt{s}$-independent term, which can cause measurable deviations in sensitive observables. The size of these deviations with respect to the SM is controlled by $g^2 s/M^2$ and it cannot be larger than a fraction of $(16\pi^2)s/M^2$, therefore, we expect small effects from new physics of mass $M \gg \sqrt{s}$. Indeed, if these effects were big, we would have already received hints at the LHC and direct production of new states would be a more suitable way to search for new physics at the muon collider. Having in mind the "unit of measurement" in Equation (6) we understand why 1% to 10% starts being an interesting level of precision to probe new physics indirectly. This is about the largest effect one can expect for new physics heavy enough to escape the direct production and be well within the approximation we make by taking perturbative values of g in the expansion parameter of our EFT in Equation (6).

3.4.1. The Size of the Higgs Boson

To be concrete we want to discuss the example of new physics indirect effects in precision studies of quantities related to the Higgs boson, and in particular to both the physical Higgs boson and the would-be Goldstone bosons eaten in the massive gauge vector bosons in the Higgs mechanism. This example highlights extremely well the power of a high energy muon collider to study the Higgs sector of the Standard Model.

The theoretical setting in which we can carry out this study is a dimension-6 EFT that extends the SM, the so-called SMEFT [92], or an equivalent EFT in which the Higgs boson is more directly involved in the new contact interactions. Although these "bases" for the EFT

can be shown to be equivalent in physical results, the SILH basis [93] is more transparent for our study as it highlights the effects on Higgs, Goldstone and gauge bosons interactions.

The dim-6 Lagrangian that extends the SM in the SILH basis has a large number of terms. Dealing with them all at once needs to carry out many measurements to constrain each contact interaction using a sensitive measurement. To reduce the complexity of this task we can approach the problem with some theoretical picture that provides rough estimates on the size of each of the many contact interactions. This amounts to image a concrete dynamic for the UV Lagrangian that gives rise to the low-energy EFT and provides us with a rough parametrization of the size of each contact interactions. The size of the contact interaction couplings can be expressed in terms of powers of the fundamental parameters of the UV Lagrangian, up to numerical factors that depend on the specific UV Lagrangian and that are not interesting to obtain just an estimate of the size of the BSM interactions. This is the so-called "power counting" which allows estimation of the size of interactions strength from a generic type of UV completion of the EFT.

In the SILH case a power counting for generic UV completion describes the possibility that the Higgs boson is not a point-like particle, but it has a finite size $\ell_H \sim 1/m_\star$ which is about the order of magnitude of the mass of heavy new physics that belongs to the UV completion of the low-energy SILH EFT. In this picture the Higgs boson is a light particle of the theory valid at and above the EFT scale and it just happens to be light enough for us to produce it and study it.

The position of the Higgs bosons is then similar to the position of the pions in the world of hadrons. They are light enough that one can study pion scattering (or Higgs boson physics) even if the available energy is limited below the mass of the first ρ meson and the other heavier hadrons. Pions are therefore both part of a low-energy EFT, the so-called sigma model of pions, but are also the first of a long list of hadrons, which eventually can be understood all as low-energy manifestations of more fundamental quarks and gluons. The lightness of the pions can be understood from the fact that they are Goldstone bosons of an underlying symmetry of QCD, broken by the quark masses. Thus, at least when the symmetry is not too badly broken, pions and other kind of Goldstone bosons are expected to be lighter than other states.

The picture of the SILH is to imagine the Higgs boson is a light composite particle, like the pions that emerges as pseudo-Nambu–Goldstone boson of the symmetry breaking pattern of the UV completion of our low-energy EFT. The study of precision observables involving the Higgs bosons and the eaten Goldstone bosons of the SM can be seen as the study of pions in search for the evidence of indirect effects of heavier ρ mesons. The mass of said ρ meson can be seen as the energy scale of momentum transferred at which we start probing distances so short that the structure of the Higgs boson starts to emerge, fully displaying its finite size.

To probe the size of the Higgs boson a very effective strategy consists of studying Higgs and Goldstone bosons scattering in all possible production processes. The effects of the finite size of the Higgs boson are enhanced by the momentum transferred in the reactions, therefore this study has a clear demand for high-energy. Nevertheless, several collisions to measure rates with sufficient precision is necessary to create bounds. In Ref. [72] the number of events for the reaction Zh expected for luminosity Equation (5) has been translated into an expected bound on the size of the Higgs boson for generic $\sqrt{s}$ muon collider. This bound corresponds to the orange line in Figure 5 on which we highlighted center-of-mass energies 3 TeV, 10 TeV and two "10 + TeV" options at 30 TeV and 100 TeV. The result that a high-energy muon collider can attain on the size of the Higgs boson clearly exceed the reach of other future collider projects, as reported by dashed lines.
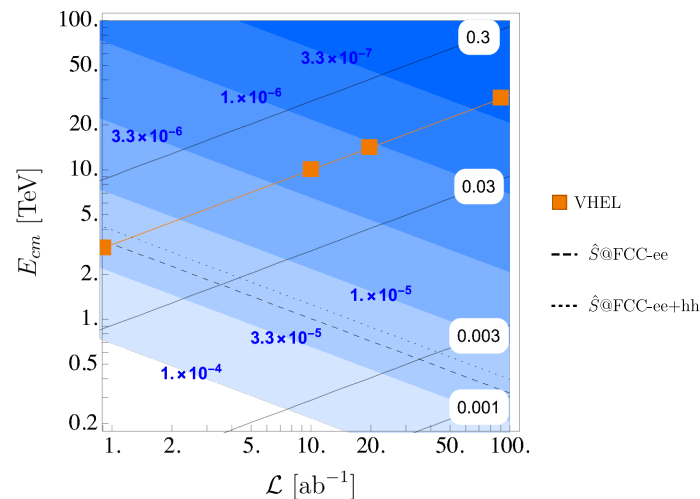
Figure 5. Lower-bounds on $m_\star = 1/\ell_H$ expressed as upper bounds on $\hat{S} = (m_W/m_\star)^2$ (blue shades and labels). Dashed lines correspond to limits on the same quantity from the combination of *ee* Higgs factory and high-energy *pp* colliders *FCC*-ee an *FCC*-hh [20].

Figure 5 allows also to evaluate the bounds for different amount of luminosity. In particular, it highlights that the luminosity requirement of Equation (5) is quite close to the least possible luminosity necessary to meaningfully run this analysis. In fact, the solid black lines correspond to the size of the deviation from the SM *Zh* total rate at which one has to be sensitive to create a bound on $m_\star$ as strong as what indicated by the shade of blue in the figure. The orange line for our baseline luminosity runs parallel to these lines of iso-S/B and corresponds to be sensitive to around 10% deviations at 95% CL. Thus, if we imagine to run the same energy with lower luminosity we would be effectively probing theories for which the EFT expansion parameter Equation (6) has grown to be close to $O(1)$, hence in a regime in which the EFT may not be valid. A simple way to fall in this case is to reduce the mass of the new physics in Equation (6), which eventually leads to $M < \sqrt{s}/2$ and thus makes the indirect search strategy no longer meaningful. All in all, if we want to pursue indirect new physics searches we need to push the energy of the machine, as to profit from the growth with energy of the new physics effects, but at the same time, we need to keep a target luminosity around Equation (5), or else the whole strategy of indirect new physics searches collapses. In this eventuality the high-energy muon collider would be a machine suitable for direct new physics exploration, up to its kinematical limit $\sqrt{s}/2$ for pair production, and with no meaningful sensitivity whatsoever to new physics heavier than that.

A more complete analysis using other processes that involve Goldstone and Higgs bosons has been carried out in Ref. [72], which has analyzed hh, W^+W^-, W^+W^-h as well as *Zh* production. The results for the question on the size of the Higgs boson in some of these processes depends on the strength on the interactions in the BSM theory that completes the SM at the scale around $m_\star$, therefore we give combined results in a plane $(m_\star, g_\star)$ in Figure 6. Additionally, in this more refined setting it is clear that the high-energy muon collider options in the multi-TeV regime can improve by orders of magnitude our knowledge of the point-like nature of the Higgs boson. Thus, a high-energy muon collider operating at 10 TeV can be said to be a magnifying glass a factor above 10 more powerful than even the most powerful traditional colliders in discussion in the future collider landscape.
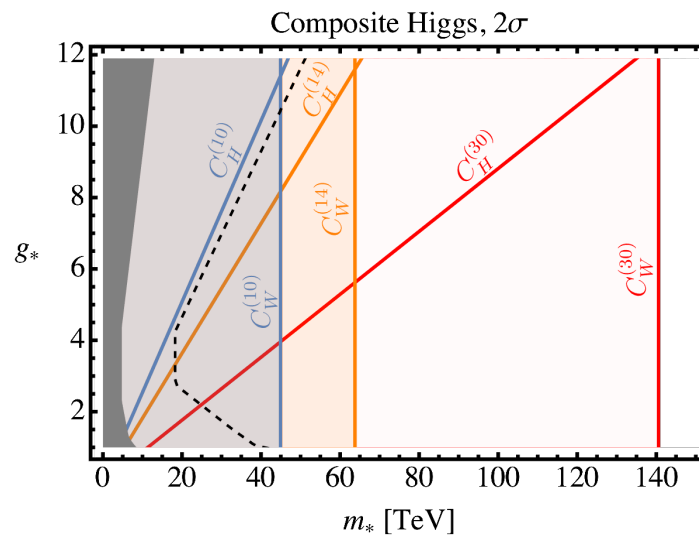
Figure 6. Bounds from Ref. [72] on the size of the Higgs bosons $\ell_H \simeq 1/m_\star$ from a 10 TeV (blue), 14 TeV (orange), 30 TeV (red) $\mu^+\mu^-$ collider using the luminosity Equation (5). The vertical lines are from di-boson and multi-boson production (e.g., W^+W^-, Zh, W^+W^-h). Diagonal lines are from hh production. Bounds con $m_\star$ depend on a generic coupling $g_\star$ as suggested by the SILH power counting. The dashed line corresponds to the limits projected for the CLIC 3 TeV stage [20]. The solid shade corresponds to the bounds from HL-LHC [20].

For completeness we remark that other bounds on the same plane can be created if the top quark is also a composite particle with a finite size, as studied in Refs. [65,75]. These bounds give even more support to the high-energy muon collider as a most powerful tool to study the Higgs boson and top quark nature as elementary particles.

3.5. Copious Production of SM States

The great fluxes of effective SM gauge bosons radiated off the beams implies that SM final states with invariant mass $\sqrt{\hat{s}} \ll \sqrt{s}$ can be produced very abundantly. Very interestingly, these processes have cross-section that grows logarithmically in this regime

$$\sigma(VBF \to SM) \simeq O(1)\,\text{pb} \cdot \log\left(\frac{\sqrt{s}/\text{TeV}}{\sqrt{\hat{s}}/0.1\text{TeV}}\right), \tag{7}$$

where the O(1) factor accounts for the different values of the fluxes of the type of boson considered in the fusion. Of course, when multiple boson fusion channels are available this estimate must be adjusted, e.g., $WW \to h$, depending on the type of analysis one has in mind, might be augmented by $ZZ, Z\gamma, \gamma\gamma \to h$ if one is not tracking the presence of forward muons in the computation of a total Higgs boson rate. Similarly, the production of colored particles or particles with spin can change the multiplicity of final states and the total rate will reflect the increased multiplicity of states.

Despite Equation (7) is only a rough estimate of the rate of producing relatively light SM states, it helps greatly to understand the potential of a high-energy muon collider in the search of new physics over the so-called intensity frontier.

3.5.1. A Giga-Higgs Boson Program

Following a luminosity scaling from the baseline Equation (5) we can anticipate a total production of Higgs bosons in the ballpark of a fraction of a billion, e.g., assuming 100 ab^{-1} at a 30 TeV collider and $\sigma_h \simeq 1.2$ pb.

Such large number of Higgs bosons produced at a high-energy muon collider qualifies the machine as a Higgs boson factory. Indeed, it is expected to produce 100 times the number of Higgs bosons considered for the most advanced low-energy "Higgs factories", such as CEPC or *FCC*-ee operating at $\sqrt{s} = 240$ GeV.

The large number of Higgs bosons expected at the high-energy muon collider will enable studies of the Higgs boson branching ratios in rare decay modes with unprecedented precision, e.g., $h \to \mu\mu$, $h \to \gamma\gamma$ and $h \to \gamma Z$ could be measured at, or even below, the 1% precision level. Being rare decay modes, new physics can be more visible in these channels.

Furthermore, new exotic rare decay modes of the Higgs boson can be searched for with a potential of being sensitive to ultra-rare decay modes down to $BR \simeq 10^{-7}$.

Of course, to achieve these results, it will be key to have sufficiently hermetic detectors or put in place suitable detectors dedicated to this kind of physics. In Figure 7 we can observe how going towards higher energies the bulk of the Higgs boson production tends to shift towards the beam pipe. Indeed, at a 30 TeV muon collider roughly half the Higgs bosons would be produced at large pseudo-rapidity $\eta_h > 2.5$. Efforts have already started [84] to study the detector performance for a moderately high-energy muon collider in the few-TeV ballpark. Continuing work [94] on detector performance under the International Muon Collider Design Study [95] has shown these early encouraging results can be further improved. Phenomenological studies [78] have concluded that it is possible to measure the hVV couplings using signatures with one Higgs boson plus unobserved forward beam remnants, e.g., neutrinos from the WBF Higgs production. Judiciously requiring the presence of a forward muon in the detector acceptance, the combination of the measured rates with and without this requirement allows the disentangled extraction of the hZZ and hWW couplings.
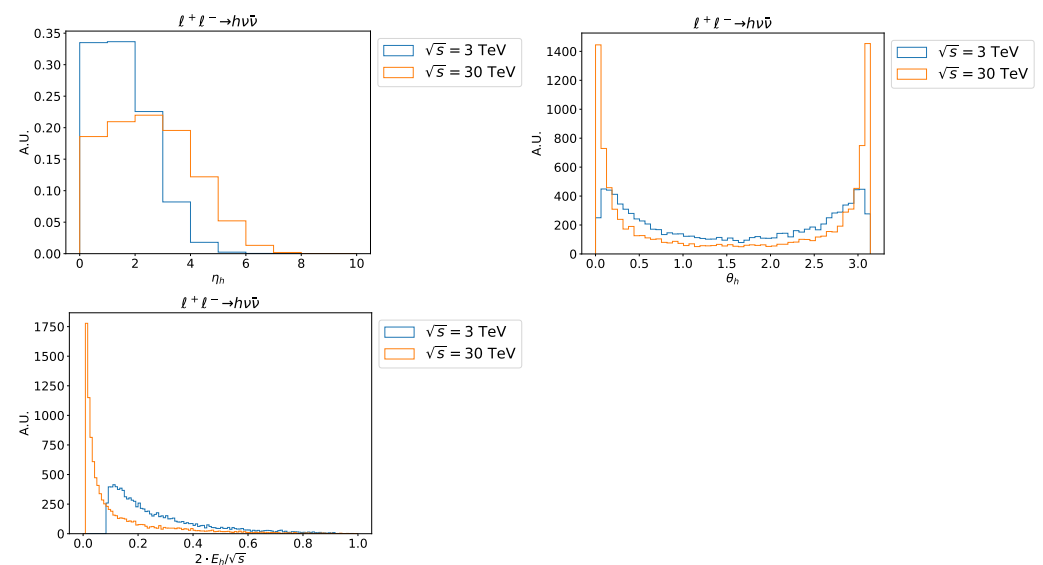

Figure 7. Higgs boson direction (as angle θ or pseudo-rapidity η) and energy distributions in the laboratory frame for $\ell^+\ell^- \to \nu\bar{\nu}h$.

Extraction of the triple and quadruple Higgs boson couplings as well as the gauge-Higgs quartic HHVV have been studied in Refs. [78,83]. Remarkably, the trilinear Higgs coupling can be extracted with a precision of around a few percent and the $hhWW$ coupling with precision around 10^{-3}, while the four h coupling can be extracted with a precision around 50%, if the hhh couplings is assumed to be as predicted in the SM.

Considering only SM final states, a global analysis of the Higgs couplings extraction from the abundant production in VBF at a multi-TeV muon collider [62] has shown that the large number of Higgs bosons produced can lead to a sub-permil determination of the hWW coupling and to percent or sub-percent precision on the other couplings, including couplings involved in rare loop decay modes such as the $hZ\gamma$ coupling, and the bottom quark and muon Yukawa coupling.

3.5.2. A Mega-Top Quark Program

Besides being a Higgs boson factory, a high-energy muon collider can be—at the same time and under the same machine operating conditions—a very effective top quark factory as well.

Low-Energy Top Quarks

The inclusive production of top quarks is dominated by associated production with a pair of neutrinos which yields low-boost top quarks pairs. The total cross-section is about constant 20–30 fb from 3 to 30 TeV, and is clearly a lot lower than a low-energy lepton collider, where fraction of pb can be attained. However, thanks to the luminosity Equation (5) expected at a high-energy muon collider the number of top quarks produced by *W* fusion can be comparable, and even larger, than what can be attained at machines operating around the threshold for the Drell–Yan production such as e^+e^- machines at proposed 350, 380 or 500 GeV dedicated stages.

A comparison of cross-sections and total number of top quarks produced is reported in Table 3. The large flux of partons that can produce top quark pairs is clearly sufficient to pursue a full fledge program "at the pole" of the top quark with similar measurements as those considered for other lepton colliders with dedicated top quark physics stages [96–99].

Table 3. Top quark production cross-section in Drell–Yan (**A**) and *W* boson fusion (**B**) at $\sqrt{s} = 0.5$ TeV, 3 TeV, 30 TeV. These numbers are obtained at LO in perturbation theory using MadGraph5_aMC@NLO [100]. The luminosities used are those following Equation (5) for 30 TeV, whereas we use projected luminosities for top quark factory operation of ILC at 0.5 TeV [101] and CLIC 3 TeV [90]. Radiative corrections and beam energy spreads should be taken into account in a realistic setup but are not expected to change the overall picture (e.g., at 3 TeV $\sigma(\ell^+\ell^- \to t\bar{t}) = 25$ fb if radiative corrections are included [96]).

(A)			
$\sqrt{s}$	$\sigma(\ell^+\ell^- \to t\bar{t})$	$\mathcal{L}$	$\sigma \cdot \mathcal{L}$
0.5 TeV	548 fb	4/ab	2.2M
3 TeV	19 fb	2.5/ab	47K
30 TeV	0.19 fb	90/ab	17K

(B)			
$\sqrt{s}$	$\sigma(\ell^+\ell^- \to \nu\nu t\bar{t})$	$\mathcal{L}$	$\sigma \cdot \mathcal{L}$
0.5 TeV	0.23 fb	4/ab	0.9K
3 TeV	5.4 fb	5/ab	27K
30 TeV	31 fb	90/ab	2.7M

High-Energy Top Quarks

The increase of luminosity with energy we have assumed in Equation (5) guarantees an approximatively constant number of top quarks produced from large momentum transfer processes such as $2 \to 2$ scattering $\ell^+\ell^- \to t\bar{t}$. Therefore, it is possible to carry out measurements at large momentum transfer keeping statistical uncertainty constant even if the collider energy considered varies. With such provision we can quickly estimate the reach of a high-energy muon collider in a similar way to what we have seen for di-boson processes. Following the di-boson path [72] we can put very stringent bounds on contact interactions that involve top quarks and give rise to effects that grow with momentum transfer. In this aspect a high-energy muon collider has an increased potential to probe new physics at high-energy and it essentially offers the best reach for a collider of same beam–beam center-of-mass energy. Preliminary results presented in Ref. [65] confirm these estimates, but more refined studies are needed.

While a dedicated study of the reach for new physics using high-momentum transfer $\ell^+\ell^- \to t\bar{t}$ production is not yet available, we can quickly estimate the expected perfor-

mance extrapolating from CLIC 3 TeV studies. Bremsstrahlung and ISR effects are different for a muon collider and a e^+e^- linear collider, still we can obtain a reliable estimate of the ballpark of the reach of a simple angular distribution study of new physics effects in DY production. A 30 TeV muon collider can be sensitive to new physics from mass scales well in excess of 100 TeV.

Further Production Modes and Measurements: $e^+e^- \to t\bar{t}h + X$ **the Yukawa Coupling y_t and More**

Exploiting the large center-of-mass energy, it is possible to produce richer final states than the simple $t\bar{t}$. For instance, it is possible to obtain the $t\bar{t}h$ final state, which is sensitive to the top quark Yukawa coupling and is characterized by large momentum transfer.

This process can give a direct measurement of y_t with a precision around a few percent. Although the precision on y_t per se is not much different from what can be obtained at less energetic colliders, e.g., the 3 TeV stage of CLIC, the fact that this measurement is characterized by a much larger momentum transfer makes it much more sensitive to possible new physics contributions. A through study of the sensitivity of $t\bar{t}h$ to new physics in a clean EFT language is still missing; however, we can expect that this measurement will be very sensitive to contact interactions, thanks to the benefit from running at high energy.

At the high-energy muon collider, it will be possible to produce top quarks and Higgs bosons in even more complex final states such as $t\bar{t}h\nu\bar{\nu}$. Additionally, this process is sensitive to the Yukawa coupling of the top quark, but is characterized by the typical momentum transfer of the WBF processes, hence it is not going to be a most powerful probe of contact interactions involving the Higgs boson and the top quark. Putting this process together with the high-momentum transfer $t\bar{t}h$ we expect to be able to constrain both new physics effects that are magnified by the momentum transfer, hence are suppressed by an EFT expansion parameter similar to Equation (6), and those that are insensitive to the momentum transfer, e.g., those which can be cast as pure shifts of SM parameters.

For a quick estimate of the power of these processes in constraining new physics we can look at 30 TeV muon collider rates reported in Table 4 and the resulting statistical uncertainties on these rates. Keeping in mind that high-momentum transfer $t\bar{t}h$ rates should be used to create bounds on effects of new physics that grow with energy, we can see how at a 30 TeV machine the two classes of processes have a similar statistical uncertainty, hence at this large center-of-mass energies it is possible to simultaneously carry out new physics searches and create meaningful bounds using both types of processes.

Table 4. Expected rates for $t\bar{t}h + X$ reactions and an estimate on the sensitivity to energy-independent effects, such as a shift in the Yukawa coupling of the top quark.

$\sqrt{s}$	$\sigma(\ell^+\ell^- \to t\bar{t}h)$	$\mathcal{L}$	$\sigma \cdot \mathcal{L}$	$\frac{\delta\sigma}{\sigma}$ at 68% CL	$\frac{\delta y_t}{y_t}$ at 68% CL
30 TeV	7 ab	90/ab	630	4.0%	2.0%
	$\sigma(\ell^+\ell^- \to t\bar{t}h\nu\nu)$	$\mathcal{L}$	$\sigma \cdot \mathcal{L}$	$\frac{\delta\sigma}{\sigma}$ at 68% CL	$\frac{\delta y_t}{y_t}$ at 68% CL
30 TeV	100 ab	90/ab	9000	1%	0.5%

All in all, it is possible to imagine a rich physics case for the study of new physics involving the top quark and the Higgs boson at the high-energy muon collider. Learning the results sketched above a larger set of processes can be imagined for an extended program on the top and bottom quarks and Higgs boson sector involving $b\bar{b} + X, b\bar{b}h + X, tb + X$, and $tbh + X$ processes. Preliminary results on this enlarged set of processes [102] indicate that they have a constraining power similar to di-boson processes on new physics scenarios where the Higgs boson and the third-generation quarks are not elementary point-like states.

4. Conclusions

The Higgs boson is a cornerstone of the Standard Model of particle physics, as it provides a concrete realization of the mechanism of spontaneous symmetry breaking needed to separate electromagnetic and weak gauge interactions. The Higgs boson is also a unique and singular object in the present formulation of the SM. In fact, it is the only Lorentz scalar in the model and needs to be exactly point-like for the model to be consistent. At the same time, the Higgs boson mass and its properties have a remarkable sensitivity to the existence of new heavy states, whose mass acts as a source of destabilization of the weak scale. With such unique role in the SM and special properties in QFT in general, the Higgs boson is a most important target for studies to be carried out at future particle physics facilities.

In this contribution we have highlighted the possible studies that a low-energy muon collider might enable a better understanding of the nature of the Higgs boson. We have outlined significant challenges for the use of data coming from Higgs bosons produced from resonant annihilation of muons beams. The quality of the beam, and in particular its energy spread, turns out to be a key parameter to assess the outcome of Higgs boson factory at the pole. If a machine at the Higgs boson pole could be realized with relative beam energy spread $O(3 \times 10^{-5})$, and a few fb^{-1} integrated luminosity accumulated, the results on the Higgs boson couplings would bring a significant improvement over the most optimistic HL-LHC projections. In the landscape of future colliders and their performance on the determination of Higgs boson properties these improvements generally fall short compared to other projects. However, it should be remarked that a Higgs boson factory from resonant muon annihilation might provide the best measurement of the Higgs boson coupling to muons and might be one of the few ways, if not the only one, to directly measure the Higgs boson width with good precision.

In the second part of our contribution, we have discussed the possibility of using a high-energy muon collider to study the Higgs boson and in general the Higgs sector and the physics BSM associated with it. We have outlined a physics program that can be pursued at a multi-TeV muon collider by leveraging both high rate reactions at low momentum transfer, such as the vector boson fusion production of Higgs bosons and other SM states, and the high-momentum transfer reactions such as direct Drell–Yan annihilation processes into SM states or possible BSM final states. Concerning the physics of the Higgs boson we have highlighted the possibility to study contact interactions involving the Higgs boson or longitudinal gauge bosons (or both) as a mean to study new physics in the Higgs sector. We have discussed how this search for new physics effects demands the operation of such a multi-TeV machine with sufficient luminosity to be able to study at the few-percent level the total rate of the least abundant SM Drell–Yan process, e.g., $\mu^+\mu^- \rightarrow Zh$.

A machine designed to collect around 10 ab^{-1} at 10 TeV center-of-mass energy can potentially probe new physics related to the breaking of the electroweak symmetry and the Higgs boson up to mass scales just short of 100 TeV.

The luminosity requirement outlined above in Equation (5) for the investigation of new physics related to the Higgs boson would also enable a host of investigation for contact interactions of SM states that can be generated by new physics. Therefore, the achievement of these luminosity targets would place experiments run at the high-energy muon collider in a position to be sensitive to many new physics scenarios. Furthermore, the collection of such large luminosity would enable the precision study of SM states produced in low momentum transfer reactions from a dataset of unprecedented size and the unique feature of being produced from purely electroweak reactions. These studies of SM states would complement beautifully with the study of contact interactions from new physics, essentially "multiplexing" the physics case of the muon collider.

Should the luminosity requirement indicated above not be met, the high-energy muon collider remains a fantastic machine to explore the energy frontier. In fact, it provides a clean environment to study the results of high-energy collisions and at the same time can probe very large mass scale, thus putting together the best of the e^+e^- and pp colliders

features. The direct search of new heavy particles is a key ability of a high-energy muon collider, as it can probe heavy new physics charged under electroweak gauge interactions, which is ubiquitous in new physics models. Thanks to the clean collision environment a high-energy muon collider operating even 2 orders of magnitude below the luminosity requirement discussed for indirect new physics searches would be able to discover new particles up to about $\sqrt{s}/2$, hence swiping the whole range from the HL-LHC limits to the multi-TeV mass range.

Although the direct search of new physics states is an exciting and potentially rewarding program, it is very important to stress that designs aimed at the luminosity requirement outlined for indirect searches of new physics may be even more rewarding and far reaching. The consequence of establishing the feasibility of a baseline luminosity

$$\mathcal{L} = 10\,\mathrm{ab}^{-1}\left(\frac{\sqrt{s}}{10\,\mathrm{TeV}}\right)^2,$$

would be momentous. In fact, by going at higher energies while increasing luminosity it would lead to a path of systematically improving the results described above testing new physics mass scale that grow linearly with center-of-mass energy.

It is important to stress that this possibility is unique to muon colliders. In fact, at variance with circulating and linear electron and positron beams, muon beams can be manipulated so that it is in principle possible to reach a luminosity per unit wall-plug power that grows as the beam energy grows [10,28]. Therefore, muon beams allow the entertainment of the idea of collisions at even higher center-of-mass energies in the tens of TeV. Thanks to the relatively low power cost "per TeV" center-of-mass energy of these machines we can reasonably imagine extending the high-energy muon collider physics program at higher energies with instantaneous luminosity that grow as s, thus keeping a fixed amount of recorded events for the simplest Drell–Yan annihilations. Along this line we can imagine an upgrade path for the investigations of new physics related to the Higgs boson that for a center-of-mass energy of 30 TeV would be probing mass scales of new physics in the range of hundreds of TeV.

References

1. Budker, G.I. Accelerators and colliding beams. *Conf. Proc. C* **1969**, *690827*, 33–39.
2. Budker, G.I. Research work on the colliding beams of the Novosibirsk Institute of Nuclear Physics (present state of experiments and perspectives). *AIP Conf. Proc.* **1996**, *352*, 5.
3. Skrinsky, A.N. Polarized muon beams for muon collider. *Nucl. Phys. B Proc. Suppl.* **1996**, *51*, 201–203. [CrossRef]
4. Neuffer, D. Multi-TeV muon colliders. *AIP Conf. Proc.* **1987**, *156*, 201–208. [CrossRef]
5. Blondel, A.; Ellis, J.R.; Autin, B. Prospective Study of Muon Storage Rings at CERN. In *CERN Yellow Reports: Monographs*; CERN: Geneva, Switzerland, 1999. [CrossRef]
6. Ankenbrandt, C.M.; Atac, M.; Autin, B.; Balbekov, V.I.; Barger, V.D. Status of muon collider research and development and future plans. *Phys. Rev. ST Accel. Beams* **1999**, *2*, 081001. [CrossRef]

7.	Geer, S. Muon Colliders and Neutrino Factories. *Ann. Rev. Nucl. Part. Sci.* **2009**, *59*, 347–365. [CrossRef]

8.	Rubbia, C. A complete demonstrator of a muon cooled Higgs factory. *arXiv* **2013**, arXiv:1308.6612.

9.	Palmer, R.B. Muon Colliders. *Rev. Accel. Sci. Technol.* **2014**, *7*, 137–159. [CrossRef]

10.	Boscolo, M.; Delahaye, J.P.; Palmer, M. The future prospects of muon colliders and neutrino factories. *Rev. Accel. Sci. Technol.* **2019**, *10*, 189–214. [CrossRef]

11.	Barger, V.D.; Berger, M.S.; Gunion, J.F.; Han, T. Higgs Boson physics in the s channel at $\mu^+\mu^-$ colliders. *Phys. Rept.* **1997**, *286*, 1–51. [CrossRef]

12.	Long, K.; Lucchesi, D.; Palmer, M.; Pastrone, N.; Schulte, D.; Shiltsev, V. Muon colliders to expand frontiers of particle physics *arXiv* **2020**, arXiv:2007.15684.

13.	ATLAS Collaboration; Aad, G.; Abajyan, T.; Abbott, B.; Abdallah, J.; Khalek, S.A.; Abdelalim, A.A.; Abdinov, O.; Aben, R.; Abi, B.; et al. Observation of a new particle in the search for the Standard Model Higgs boson with the ATLAS detector at the LHC. *Phys. Lett. B* **2012**, *716*, 1–29. [CrossRef]

14.	CMS Collaboration; Chatrchyan, S.; Khachatryan, V.; Sirunyan, A.M.; Tumasyan, A.; Adam, W.; Aguilo, E.; Bergauer, T.; Dragicevic, M.; Erö, J.; et al. Observation of a New Boson at a Mass of 125 GeV with the CMS Experiment at the LHC. *Phys. Lett. B* **2012**, *716*, 30–61. [CrossRef]

15.	Robson, A.; Burrows, P.N.; Catalan Lasheras, N.; Linssen, L.; Petric, M.; Schulte, D.; Sicking, E.; Stapnes, S.; Wuensch, W. The Compact Linear e$^+$e$^-$ Collider (CLIC): Accelerator and Detector. *arXiv* **2018**, arXiv:1812.07987.

16.	Abada, A.; Abbrescia, M.; AbdusSalam, S.S.; Abdyukhanov, I.; Fernandez, J.A.; Abramov, A.; Aburaia, M.; Acar, A.O.; Adzic, P.R.; Agrawal, P.; et al. FCC-ee: The Lepton Collider: Future Circular Collider Conceptual Design Report Volume 2. *Eur. Phys. J. ST* **2019**, *228*, 261–623. [CrossRef]

17.	Greco, M.; Han, T.; Liu, Z. ISR effects for resonant Higgs production at future lepton colliders. *Phys. Lett. B* **2016**, *763*, 409–415. [CrossRef]

18.	CLIC and CLICdp Collaborations. The Compact Linear e$^+$e$^-$ Collider (CLIC): Accelerator and Detector. *arXiv* **2018**, arXiv:1812.07987.

19.	Ruth, R.D. *CTF3 Design Report*; SLAC: Stanford, CA, USA, 2003. Available online: http://cds.cern.ch/record/747483 (accessed on 13 March 2003).

20.	European Strategy for Particle Physics Preparatory Group. Physics Briefing Book—Input for the European Strategy for Particle Physics Update 2020. In *Physics Briefing Book*; CERN: Geneva, Switzerland, 2019.

21.	Shiltsev, V. Will There Be Energy Frontier Colliders After LHC? In Proceedings of the 38th International Conference on High Energy Physics (ICHEP 2016), Chicago, IL, USA, 3–10 August 2016.

22.	Shiltsev, V. Considerations On Energy Frontier Colliders After LHC. *arXiv* **2017**, arXiv:1705.02011.

23.	The CEPC Study Group. CEPC Conceptual Design Report: Volume 2—Physics and Detector. *arXiv* **2018**, arXiv:1811.10545.

24.	The CEPC Study Group. CEPC Conceptual Design Report: Volume 1—Accelerator. *arXiv* **2018**, arXiv:1809.00285.

25.	Benedikt, M.; Blondel, A.; Brunner, O.; Capeans Garrido, M.; Cerutti, F.; Gutleber, J.; Janot, P.; Jimenez, J.M.; Mertens, V.; Milanese, A.; et al. *Future Circular Collider—Volume 2—The Lepton Collider FCC-ee Conceptual Design Report*; Technical Report CERN-ACC-2018-0057; CERN: Geneva, Switzerland, 2018.

26.	Barna, D. High field septum magnet using a superconducting shield for the Future Circular Collider. *Phys. Rev. Accel. Beams* **2017**, *20*, 041002. [CrossRef]

27.	Barna, D.; Novak, M.; Brunner, K.; Petrone, C.; Atanasov, M.; Feuvrier, J.; Pascal, M. NbTi/Nb/Cu multilayer shield for the superconducting shield (SuShi) septum. *arXiv* **2018**, arXiv:1809.04330v1.

28.	Delahaye, J.P.; Diemoz, M.; Long, K.; Mansoulié, B.; Pastrone, N.; Rivkin, L.; Schulte, D.; Skrinsky, A.; Wulzer, A. Muon Colliders. *arXiv* **2019**, arXiv:1901.06150.

29.	Bernardini, C.; Corazza, G.F.; Ghigo, G.; Touschek, B. The Frascati storage ring. *IL Nuovo C* **1960**, *18*, 1293–1295. [CrossRef]

30.	Cabibbo, N.; Gatto, R. Electron Positron Colliding Beam Experiments. *Phys. Rev.* **1961**, *124*, 1577–1595. [CrossRef]

31.	Bernardini, C. AdA: The first electron-positron collider. *Phys. Perspect.* **2004**, *6*, 156–183. [CrossRef]

32.	Schmueser, P. Superconductivity in high energy particle accelerators. *Prog. Part. Nucl. Phys.* **2002**, *49*, 155–244. [CrossRef]

33.	Marriner, J. Stochastic cooling overview. *Nucl. Instrum. Methods Phys. Res. Sect. A* **2004**, *532*, 11–18. [CrossRef]

34.	MICE Collaboration. Demonstration of cooling by the Muon Ionization Cooling Experiment. *Nature* **2020**, *578*, 53–59. [CrossRef]

35.	Rubbia, C. Further searches of the Higgs scalar sector at the ESS. *arXiv* **2019**, arXiv:1908.05664.

36.	Antonelli, M.; Boscolo, M.; Di Nardo, R.; Raimondi, P. Novel proposal for a low emittance muon beam using positron beam on target. *Nucl. Instrum. Meth. A* **2016**, *807*, 101–107. [CrossRef]

37.	Amapane, N.; Antonelli, M.; Anulli, F.; Ballerini, G.; Bandiera, L.; Bartosik, N.; Bertolin, A.; Biino, C.; Blanco-Garcia, O.R.; Boscolo, M.; et al. LEMMA approach for the production of low-emittance muon beams. *Nuovo Cim. C* **2020**, *42*, 259. [CrossRef]

38.	Augustin, J.E.; Boyarski, A.M.; Breidenbach, M.; Bulos, F.; Dakin, J.T.; Feldman, G.J.; Fischer, G.E.; Fryberger, D.; Hanson, G.; Jean-Marie, B.; et al. Discovery of a Narrow Resonance in e^+e^- Annihilation. *Phys. Rev. Lett.* **1974**, *33*, 1406–1408. [CrossRef]

39.	Greco, M.; Pancheri-Srivastava, G.; Srivastava, Y. Radiative Corrections for Colliding Beam Resonances. *Nucl. Phys. B* **1975**, *101*, 234–262. [CrossRef]

40.	Greco, M.; Pancheri-Srivastava, G.; Srivastava, Y. Radiative Corrections to $e^+e^- \rightarrow \mu^+\mu^-$ Around the Z^0. *Nucl. Phys. B* **1980**, *171*, 118; Erratum in **1982**, *197*, 543. [CrossRef]

41. Nicrosini, O.; Trentadue, L. Soft Photons and Second Order Radiative Corrections to $e^+e^- \to Z^0$. *Phys. Lett. B* **1987**, *196*, 551. [CrossRef]

42. Greco, M. On the study of the Higgs properties at a muon collider. *Mod. Phys. Lett. A* **2015**, *30*, 1530031. [CrossRef]

43. Jadach, S.; Kycia, R.A. Lineshape of the Higgs boson in future lepton colliders. *Phys. Lett. B* **2016**, *755*, 58–63. [CrossRef]

44. Kuraev, E.A.; Fadin, V.S. On Radiative Corrections to e^+e^- Single Photon Annihilation at High-Energy. *Sov. J. Nucl. Phys.* **1985**, *41*, 466–472.

45. Blas, J.D.; Cepeda, M.; D'Hondt, J.; Ellis, R.K.; Grojean, C.; Heinemann, B.; Maltoni, F.; Nisati, A.; Petit, E.; Rattazzi, R.; et al. Higgs Boson Studies at Future Particle Colliders. *arXiv* **2019**, arXiv:1905.03764v1.

46. Han, T.; Liu, Z. Potential precision of a direct measurement of the Higgs boson total width at a muon collider. *Phys. Rev. D* **2013**, *87*, 033007. [CrossRef]

47. Conway, A.; Wenzel, H. Higgs Measurements at a Muon Collider. *arXiv* **2013**, arXiv:1304.5270v1.

48. Janot, P. Higgs Properties at Circular Lepton Colliders. CERN Faculty Meeting June 1st 2018. Available online: https://indico.cern.ch/event/716380/ (accessed on 1 March 2021).

49. Liu, Z. Physics at Higgs Factories. Available online: https://indico.cern.ch/event/969815/contributions/4098170/ (accessed on 1 March 2021).

50. An, F.; Bai, Y.; Chen, C.; Chen, X.; Chen, Z.; da Costa, J.G.; Cui, Z.; Fang, Y.; Fu, C.; Gao, J.; et al. Precision Higgs Physics at CEPC. *arXiv* **2018**, arXiv:1810.09037v2.

51. Benedikt, M.; Blondel, A.; Brunner, O.; Capeans Garrido, M.; Cerutti, F.; Gutleber, J.; Janot, P.; Jimenez, J.M.; Mertens, V.; Milanese, A.; et al. Future Circular Collider—The Lepton Collider (FCC-ee)—European Strategy Update Documents. 2019. Available online: https://cds.cern.ch/record/2653669 (accessed on 1 March 2021).

52. Abada, A.; Abbrescia, M.; AbdusSalam, S.S.; Abdyukhanov, I.; Fernandez, J.A.; Abramov, A.; Aburaia, M.; Acar, A.O.; Adzic, P.R.; Agrawal, P.; et al. FCC Physics Opportunities: Future Circular Collider Conceptual Design Report Volume 1. Future Circular Collider. *Eur. Phys. J. C* **2019**, 474. [CrossRef]

53. De Blas, J.; Gu, J.; Liu, Z. Understinging the Higgs Precision at Muon Collider Higgs Factory. 2021, in preparation.

54. Abramowicz, H.; Abusleme, A.; Afanaciev, K.; Alipour Tehrani, N.; Balázs, C.; Benhammou, Y.; Benoit, M.; Bilki, B.; Blaising, J.-J.; Boland, M.J.; et al. Higgs physics at the CLIC electron–positron linear collider. *Eur. Phys. J.* **2017**, *C77*, 475. [CrossRef]

55. Dainese, A.; Mangano, M.; Meyer, A.B.; Nisati, A.; Salam, G.; Vesterinen, M.A. Report on the Physics at the HL-LHC, and Perspectives for the HE-LHC. *CERN Yellow Rep. Monogr.* **2019**, *7*. [CrossRef]

56. Ohnishi, Y.; Abe, T.; Adachi, T.; Akai, K.; Arimoto, Y.; Ebihara, K.; Egawa, K.; Flanagan, J.; Fukuma, H.; Funakoshi, Y.; et al. Accelerator design at SuperKEKB. *PTEP* **2013**, *2013*, 03A011. [CrossRef]

57. Rossi, L.; Badel, A.; Bajko, M.; Ballarino, A.; Bottura, L.; Dhallé, M.M.J.; Durante, M.; Fazilleau, P.; Fleiter, J.; Goldacker, W.; et al. The EuCARD-2 Future Magnets European Collaboration for Accelerator-Quality HTS Magnets. *IEEE Trans. Appl. Supercond.* **2015**, *25*, 1–7. [CrossRef]

58. Gourlay, S. Superconducting accelerator magnet technology in the 21st century: A new paradigm on the horizon? *Nucl. Instrum. Methods Phys. Res. Sect. A* **2018**, *893*, 124–137. [CrossRef]

59. The European Strategy Group. *Deliberation Document on the 2020 Update of the European Strategy for Particle Physics*; Technical Report CERN-ESU-014; CERN: Geneva, Switzerland, 2020. [CrossRef]

60. The European Strategy Group. *2020 Update of the European Strategy for Particle Physics*; Technical Report CERN-ESU-013; CERN: Geneva, Switzerland, 2020. [CrossRef]

61. Asadi, P.; Capdevilla, R.; Cesarotti, C.; Homiller, S. Searching for Leptoquarks at Future Muon Colliders. *arXiv* **2021**, arXiv:2104.05720v1.

62. Ali, H.A.; Arkani-Hamed, N.; Banta, I.; Benevedes, S.; Buttazzo, D.; Cai, T.; Cheng, J.; Cohen, T.; Craig, N.; Ekhterachian, M.; et al. The Muon Smasher's Guide. *arXiv* **2021**, arXiv:2103.14043v1.

63. Bottaro, S.; Strumia, A.; Vignaroli, N. Minimal Dark Matter bound states at future colliders. *arXiv* **2021**, arXiv:2103.12766v1.

64. Han, T.; Ma, Y.; Xie, K. Quark and Gluon Contents of a Lepton at High Energies. *arXiv* **2021**, arXiv:2103.09844v1.

65. Serra, J. Opportunities for Studying Top Compositeness at a Muon Collider. Available online: https://indico.cern.ch/event/1008639/ (accessed on 1 March 2021).

66. Huang, G.Y.; Jana, S.; Queiroz, F.S.; Rodejohann, W. Probing the $R_{K^{(*)}}$ Anomaly at a Muon Collider. *arXiv* **2021**, arXiv:2103.01617v1.

67. Capdevilla, R.; Meloni, F.; Simoniello, R.; Zurita, J. Hunting wino and higgsino dark matter at the muon collider with disappearing tracks. *arXiv* **2021**, arXiv:2102.11292v1.

68. Han, T.; Li, S.; Su, S.; Su, W.; Wu, Y. Heavy Higgs Bosons in 2HDM at a Muon Collider. *arXiv* **2021**, arXiv:2102.08386v1.

69. Liu, W.; Xie, K.P. Probing electroweak phase transition with multi-TeV muon colliders and gravitational waves. *arXiv* **2021**, arXiv:2101.10469v1.

70. Capdevilla, R.; Curtin, D.; Kahn, Y.; Krnjaic, G. A No-Lose Theorem for Discovering the New Physics of $(g-2)_\mu$ at Muon Colliders. *arXiv* **2021**, arXiv:2101.10334v1.

71. Huang, G.Y.; Queiroz, F.S.; Rodejohann, W. Gauged $L_\mu - L_\tau$ at a muon collider. *arXiv* **2021**, arXiv:2101.04956v1.

72. Buttazzo, D.; Franceschini, R.; Wulzer, A. Two Paths Towards Precision at a Very High Energy Lepton Collider. *arXiv* **2020**, arXiv:2012.11555v1.

73. Yin, W.; Yamaguchi, M. Muon $g-2$ at multi-TeV muon collider. *arXiv* **2020**, arXiv:2012.03928v1.

74. Buttazzo, D.; Paradisi, P. Probing the muon $g − 2$ anomaly at a Muon Collider. *arXiv* **2020**, arXiv:2012.02769v1.

75. Banelli, G.; Salvioni, E.; Serra, J.; Theil, T.; Weiler, A. The Present and Future of Four Tops. *arXiv* **2020**, arXiv:2010.05915v1.

76. Craig, N.; Levi, N.; Mariotti, A.; Redigolo, D. Ripples in Spacetime from Broken Supersymmetry. *arXiv* **2020**, arXiv:2011.13949v1.

77. Gu, J.; Wang, L.T.; Zhang, C. An unambiguous test of positivity at lepton colliders. *arXiv* **2020**, arXiv:2011.03055v1.

78. Han, T.; Liu, D.; Low, I.; Wang, X. Electroweak Couplings of the Higgs Boson at a Multi-TeV Muon Collider. *arXiv* **2020**, arXiv:2008.12204v1.

79. Han, T.; Liu, Z.; Wang, L.T.; Wang, X. WIMPs at High Energy Muon Colliders. *arXiv* **2020**, arXiv:2009.11287v1.

80. Han, T.; Ma, Y.; Xie, K. High Energy Leptonic Collisions and Electroweak Parton Distribution Functions. *arXiv* **2020**, arXiv:2007.14300v2.

81. Capdevilla, R.; Curtin, D.; Kahn, Y.; Krnjaic, G. A Guaranteed Discovery at Future Muon Colliders. *arXiv* **2020**, arXiv:2006.16277v1.

82. Costantini, A.; Lillo, F.D.; Maltoni, F.; Mantani, L.; Mattelaer, O.; Ruiz, R.; Zhao, X. Vector boson fusion at multi-TeV muon colliders. *arXiv* **2020**, arXiv:2005.10289v1.

83. Chiesa, M.; Maltoni, F.; Mantani, L.; Mele, B.; Piccinini, F.; Zhao, X. Measuring the quartic Higgs self-coupling at a multi-TeV muon collider. *arXiv* **2020**, arXiv:2003.13628.

84. Bartosik, N.; Bertolin, A.; Buonincontri, L.; Casarsa, M.; Collamati, F.; Ferrari, A.; Ferrari, A.; Gianelle, A.; Lucchesi, D.; Mokhov, N.; et al. Detector and Physics Performance at a Muon Collider. *arXiv* **2020**, arXiv:2001.04431v1.

85. Ruhdorfer, M.; Salvioni, E.; Weiler, A. A Global View of the Off-Shell Higgs Portal. *arXiv* **2019**, arXiv:1910.04170.

86. Di Luzio, L.; Gröber, R.; Panico, G. Probing new electroweak states via precision measurements at the LHC and future colliders. *arXiv* **2018**, arXiv:1810.10993.

87. Buttazzo, D.; Redigolo, D.; Sala, F.; Tesi, A. Fusing Vectors into Scalars at High Energy Lepton Colliders. *arXiv* **2018**, arXiv:1807.04743.

88. Fornal, B.; Manohar, A.V.; Waalewijn, W.J. Electroweak Gauge Boson Parton Distribution Functions. *arXiv* **2018**, arXiv:1803.06347.

89. Chakrabarty, N.; Han, T.; Liu, Z.; Mukhopadhyaya, B. Radiative return for heavy Higgs boson at a muon collider. *Phys. Rev. D* **2015**, *91*, 015008. [CrossRef]

90. Robson, A.; Roloff, P. Updated CLIC luminosity staging baseline and Higgs coupling prospects. *arXiv* **2018**, arXiv:1812.01644.

91. TASSO Collaboration; Brandelik, R.; Braunschweig, W.; Gather, K.; Kirschfink, F.J.; Lü belsmeyer, K.; Martyn, H.-U.; Peise, G.; Rimkus, J.; Sander, H.G.; et al. Charge Asymmetry and Weak Interaction Effects in $e^+e^− \to \mu^+\mu^−$ and $e^+e^− \to \tau^+\tau^−$. *Phys. Lett. B* **1982**, *110*, 173–180. [CrossRef]

92. Grzadkowski, B.; Iskrzynski, M.; Misiak, M.; Rosiek, J. Dimension-Six Terms in the Standard Model Lagrangian. *JHEP* **2010**, *10*, 085. [CrossRef]

93. Giudice, G.F.; Grojean, C.; Pomarol, A.; Rattazzi, R. The strongly-interacting light Higgs. *J. High Energy Phys.* **2007**, *6*, 045. [CrossRef]

94. International Muon Collider Design Study. Physics and Detector Simulation. Available online: https://indico.cern.ch/category/13145/ (accessed on 1 March 2021).

95. International Muon Collider Design Study. Available online: https://muoncollider.web.cern.ch/ (accessed on 1 March 2021).

96. Abramowicz, H.; Alipour Tehrani, N.; Arominski, D.; Benhammou, Y.; Benoit, M.; Blaising, J.-J.; Boronat, M.; Borysov, O.; Bosley, R.R.; Božović Jelisavčić, I.; et al. Top-Quark Physics at the CLIC Electron-Positron Linear Collider. *arXiv* **2018**, arXiv:1807.02441v1.

97. Zarnecki, A.F. Top physics at CLIC and ILC. *arXiv* **2016**, arXiv:1611.04492.

98. Janot, P. Top-quark electroweak couplings at the FCC-ee. *J. High Energy Phys.* **2015**, *4*, 182. [CrossRef]

99. Janot, P. Precision measurements of the top quark couplings at the FCC. *arXiv* **2015**, arXiv:1510.09056v1.

100. Alwall, J.; Frederix, R.; Frixione, S.; Hirschi, V.; Maltoni, F.; Mattelaer, O.; Shao, H.S.; Stelzer, T.; Torrielli, P.; Zaro, M. The automated computation of tree-level and next-to-leading order differential cross sections, and their matching to parton shower simulations. *JHEP* **2014**, *7*, 79. [CrossRef]

101. Barklow, T.; Brau, J.; Fujii, K.; Gao, J.; List, J.; Walker, N.; Yokoya, K. ILC Operating Scenarios. *arXiv* **2015**, arXiv:1506.07830.

102. Franceschini, R. A global picture of BSM physics in the top quark sector at the future muon collider, in preparation.